SCIA '97

Proceedings of

The 10th Scandinavian Conference on Image Analysis

Lappeenranta, Finland, June 9-11, 1997

Volume I

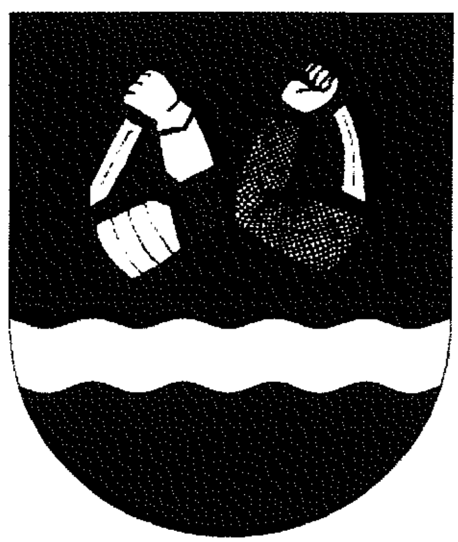

Lappeenranta University of Technology

Suomen Hahmontunnistus-
tutkimuksen Seura ry

Pattern Recognition Society
of Finland

IAPR

SCIA '97 The 10th Scandinavian Conference on Image Analysis
Lappeenranta, Finland June 9-11 1997

THE LOCALLY DEFORMABLE B-BUBBLE MODEL: AN APPLICATION TO GROWTH RING DETECTION ON FISH OTOLITHS

A. Benzinou†, H. Troadec‡, J. Le Bihan†, V. Rodin†, H. de Pontual‡, J. Tisseau†

† Ecole Nationale d'Ingénieurs de Brest
Technopôle Brest-Iroise-CP 15
29608 Brest Cedex, France
Email: benzinou@enib.fr

‡ Institut Français de Recherche pour l'Exploitation des Mers,
Centre de Brest
Laboratoire de Sclérochronologie des Animaux Aquatiques
BP 70, 29280 Plouzané, France
Email: Herve.Troadec@ifremer.fr

Abstract

One of the major problems encountered during an automatic contour detection is the lack of structure continuity perception. The usual active contour concept is a powerful tool for representing this continuity. However, existing active contour models are not suited for contour detecting in textured noisy and low contrast images. In this paper, we propose a new contour detecting algorithm that we called: the "Locally Deformable B-Bubble" model (LDBB) based on a parametric B-spline representation. The originality of this approach lies in the basic structure of the model, in the way it operates, and in the expression of a new local driving force. This model evolves by small local deformations, through its control point displacements, proportionally to a local resistance. In addition, it allows the use of high level information that constraint the bubble during its evolution. This model presents a low noise and texture sensitivity. An application to fish otolith images is presented to illustrate model efficiency.

Keywords: Active contour; Local deformation; B-spline; Otolith; Age and Growth

1. Introduction

Contour representation is usually presented as being either an edge detection and linking process or contour following. From this, we noticed numerous limitations of this traditional approach in the case of noisy, textured and poorly contrasted images. Actually, local operators used showed a great sensitivity to texture and noise induced by acquisition systems. They neither take into account global contour information and require a post-processing step to ensure contour closing. This last step suffers of a lack of global perception to organise local information detected. In order to solve those problems and to improve results on noisy images it seemed necessary to introduce, from the detection phase, contour geometric features, specially concerning its regularity. With this aim, we choose to develop a fully elastic approach.

Active contour models or "Snakes" have been introduced by Kass, Witkin & Terzopoulos [3] so as to extract features of interest in images. These models present several assets : (1) the lack of information in small regions can be overcome by the regularity of the curve which controls the global shape, (2) this model is based on an accumulation of local information which controls the local shape and hence limits noise influence, (3) a constraint energy is added to the deformation process in order to take into account the fact that the user can supply higher level information to locally restrict the contour deformation, (4) it takes into account the connexity property between the contour points along the whole curve simultaneously and therefore eliminates edge linking phase, (5) snakes are a powerful tool for shape representation which straightforwardly produces an analytical description of data. However, their practical use point out several problems linked to : (1) their numerical instability and the tendency of discretization point to agglomerate in high gradient area [1], (2) their maladjustment and even their impossibility to take into account angles and sharp curvature points [5], (3) their algorithmic complexity and model parameter fitting difficulty [9], (4) its initialisation sensitivity and its natural tendency to retraction [2]. All those features are contrary with our aims that are to reduce user operation and to reach a high process reproductibility.

Amini et al. [1] used dynamic programming for energy minimization and proposed to introduce hard constraints to avoid some of the snakes weaknesses. Actually, this approach only improves numerical stability and minimises the problem of previously evoked agglomeration. The other weaknesses remain and moreover, the algorithm is very slow and requires a very large space memory.

Cohen [2] proposed a variant to snakes, with the addition of an internal inflation force which gives them robustness to noise and to aberrant points and which minimises the influence of the starting shape during the deformation process. Cohen [2] proposed also to normalise image force field in order to decrease curve oscillations near the contour. However, this improvement enhances strongly noise and aberrant points because an aberrant point, even isolated, or a noise , even low sustains the same force than an actual contour point. Furthermore, parameter choice problem still remains and prior detection of contour points by a local detector is noise and texture sensitive because of the lack of a single image threshold.

The model described in this paper, the "Locally Deformable B-Bubble" model (LDBB), evolves by small local deformations, through its control point displacements, proportionally to local resistance, in order to find the best fit. In addition, it allows the inclusion of high level information which guides the bubble during the fitting. This model presents less sensitivity to noise and texture and hence, is more adapted to ring following in real condition.

The LDBB, is applied to the processing of otolith images. Otolith is a calcified structure of fish inner-ear which grows by concentric layers and presents growth rings that are used, as tree rings, to estimate age and growth of bony fish (figure 2). Age and growth are basic data for fish stock assessment and for most ecological studies. Otolith reading is a tedious and subjective activity which could be lightened and automated by image processing. Most of existing software, related with this topic, only propose a 1D processing of otolith image, based on the profile of a single radial line [6][8] and neglect ring continuity which is a basic criteria used by otolith expert to identify periodic marks. The development of 2D processing will be closer to human expertise and provide ring morphometric data almost unavailable up to now.

2. Local Deformation and Cubic B-spline Basic Functions

Our local scale is defined in opposition to the global process applied by previous active contour models. Each point displacement induces a local deformation that affects a portion of the curve, defined as its influence area, from which model control parameters are computed. The interest to recourse to local deformation lies in the capability to fit a large scope of shapes and in the fact that the evolution process, which controls model shape, only affects the current point. In addition, it is based on local curve information contrarily to previous approach, where shape evolution depends on the whole curve and is the same for all curve points. Hence, its allows to obtain a good algorithm robustness to noise and to react specifically for each local image context.

The algorithm proposed in this paper lies on an analytic modelisation based on cubic B-splines. Actually, this parametrization induces a slight complexity that involves a low finite number of discretization points, under the form of control points, from which the whole curve is generated. Furthermore, the curve is automatically split into portions and hence we do not need to artificially partition it. This allows to overcome discretization and parametrization problems of most active contour models. In addition, each control point only affects its four neighbouring arcs. Owing to this local control and to the basic structure of the model, which will be presented in the following section, an appropriate local deformation can be more easily generated and the model adjusted to sharp angles.

3. Basic Structure

Our approach is related to [5] only by using parametric B-spline basic functions for curve representation. LDBB is based on a simple structure which is illustrated by figure 1. It represents an object as a cubic B-spline closed curve centred on a point C and "related" to an orthonormal "reference mark" $\Re(X\,O\,Y)$. It is completely defined in terms of n control points $P_0 . P_1 . P_i . P_{n-1}$ out of which any control point P_i can only move along an axis D_i defined at $2\pi i / n$ from the X axis of the "reference" $\Re(X\,O\,Y)$.

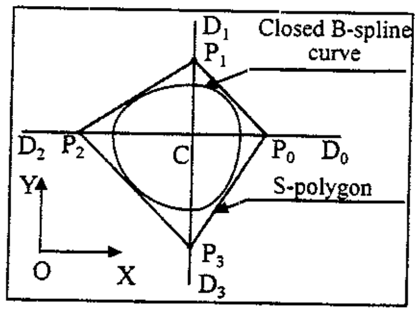

Figure 1: Example of "B-Bubble"model with 4 control points

Hence we obtain a model rigidity and a significant computing simplification. It must be noted that, by construction, the basic structure of our model, allows to avoid discretisation, instability and agglomeration problems by enforcing a distance constraint between curve points.

4. A New Local Driving Force and the Deformation Process

An initial simple curve, which may be a circle, has to be positioned first inside the object (automatically or interactively) and then the deformation process is performed iteratively. Model variables are the n positions V_i of the n control points P_i. During this iterative deformation process, each control point P_i is associated with an evolution procedure EP_i. Let t^j be a temporal variable associated with the deformation process at the iteration j. For each iteration, each control point position is individually updated according to the local external inflation force, $f(t_i^j)$. Then, the displacement quality is assessed and used to compute the next $f(t_i^j)$ to apply in order to optimise its convergence. This force determine the displacement of this control point during its future evolution :

$$V(t_i^{j+1}) = V(t_i^j) + \vec{f}(t_i^j) \bullet \vec{r_i} \qquad (1)$$

with $\vec{r_i}$ the unit vector associated with D_i axis.

Then, the next control point is moved. As a result, this new model evolves by small local deformations and is therefore less sensitive to noise and texture. From this, the model will not have any retraction ability and the curve steadiness, as well as the definition of local internal force, are linked to the choice of the basic functions. Thanks to the geometric properties of B-spline curves we do not use any explicit term of the local internal force in the expression of the local driving force.

The local external inflation force $f\left(t_i^j\right)$ is defined in order to propagate the current control point and its influence area toward the nearby object contour by detecting image intensity extrema This is similar to particle propagating in a media where their penetration vary with its resistance.

To give the explicit expression of this local inflation force, we first define the local opposite resistance $R\left(t_i^j\right)$ at control point P_i and at iteration j.

If we denote the image intensity by $I(X,Y)$ and $M_A(X,Y)$ the model area :

$$I_{image}\left(t_i^j\right) = \Sigma I(X,Y) \cap M_A(X,Y), \quad \text{for } P_i \text{ at iteration j,} \quad (2)$$

$$I_{model}\left(t_i^j\right) = \Sigma I_{max} \cap M_A(X,Y), \quad \text{for } P_i \text{ at iteration j,} \quad (3)$$

with I_{max}, the maximum intensity of a white point, then the local opposite resistance of a white area $R_W\left(t_i^j\right)$ is defined by

$$\begin{cases} R_W\left(t_i^j\right) = \left[\dfrac{I_{image}\left(t_i^j\right) - I_{image}\left(t_{i-1}^j\right)}{I_{model}\left(t_i^j\right) - I_{model}\left(t_{i-1}^j\right)}\right]^{-1}_{if\ 0<i\leq n-1} \\ R_W\left(t_0^j\right) = \left[\dfrac{I_{image}\left(t_0^j\right) - I_{image}\left(t_{n-1}^{j-1}\right)}{I_{model}\left(t_0^j\right) - I_{model}\left(t_{n-1}^{j-1}\right)}\right]^{-1}_{if\ i=0} \end{cases} \quad (4)$$

From equation (4), the local opposite resistance of a black area can be defined as :

$$\left[R_B\left(t_i^j\right)\right]^{-1} = 1 - \left[R_W\left(t_i^j\right)\right]^{-1} \quad (5)$$

Defined in this way, the local opposite resistance shows that it is convenient to define the local inflation force as follow :

$$\vec{f}\left(t_i^j\right) = \left[SMIN + (SMAX - SMIN) * \frac{1}{R\left(t_i^j\right)}\right] * \vec{r_i} \quad (6)$$

where SMAX is the maximum displacement step and SMIN is the minimum displacement step. Without any "geniricity loss", we took SMIN equals to 1. Far away from the contour, $R\left(t_i^j\right)$ is minimal and tends towards 1. The magnitude of $\vec{f}\left(t_i^j\right)$ tends then towards SMAX, giving that way a complete displacement freedom. Near the contour, $R\left(t_i^j\right)$ tends towards infinity and the magnitude of $\vec{f}\left(t_i^j\right)$, towards SMIN, decreasing the displacement freedom, in order to fix it next.

Compared with gradient potential fields, that are typically used in the previous methods, our local external force uses local texture features and is a local formulation relative to the current control point, closely linked to its speed magnitude, its acceleration and its displacement.

Furthermore, in addition to being able to path through local image intensity irregularities, its amplitude decreases gradually toward SMIN as and when it reach the contour, contrarily to gradient potential fields which induce a maximal force where we need precisely a lower one. Oscillatory phenomena are suppressed and results are more stable. Finally, as described by Cohen [2], this new local external inflation force allows to use a coarse starting curve but converges more quickly than a normalised gradient potential fields or than a uniform inflating force In case of no external force, the model is not deformed and keeps its original shape.

5. The Local Energy Minimisation and the Abort Test

In order to test whether a control point has reached the contour, control point evolution is controlled by a local energy minimisation process. This energy is defined as :

$$E\left(t_i^j\right)=\left[R\left(t_i^j\right)\right]^{-1} \tag{7}$$

Hence, this local energy, relative to a control point, is based on the area sweeped by curve deformation. A stop test is added to the process to take into account undesirable local minima of the energy function.

6. High Level Information

Our primary aim was to detect contours in textured, noisy and low contrast images. In order to avoid to get trapped into an inconsistent configuration or in an unexpected local minimum (large contour interruptions, large spots), our model is able to take into account high level information allowing to constraint curve deformation according to an *a* priori knowledge of contour geometry. Applied under the form of geometric corrections, this complementary information is essential to a correct and efficient curve evolution on otolith images. Morphogenesis is commonly used in modelisation general theory. Mathematical growth modelisation allows to describe quantitatively shape development process as well as their links with the control process [7][4].

7. Application : Growth Ring Detection in Fish Otolith Images

Application on fish otolith images, presented here, will be considered as an example of contour following and modelisation, allowing to illustrate the efficiency of the LDBB (Plaice otolith). Initialisation is done through the positioning of a circular B-spline near the otolith centre. As otolith growth is an accretionary process, ring shape modification occurs step by step during its development, inducing a shape memorisation. Ring contour detection might then be considered as a starting point for the detection of next ring. The edge contour is finally used to stop the process as well as a limit shape for high-level information. Hence, edge detection is essential and has been carefully achieved. Shape memorisation concept in otolith images will induce two kind of geometric corrections : (1) as we have associated to each control point evolution procedure a limit displacement area computation. This calculation takes into account the location of nearby points, but also the value of the maximal tension $T_{i Limit}$ that could be applied by the model on the current control point. This correction allows to unanchor a control point wrongly fixed when neighbouring points are still moving (stop on a large spot), or to stop an isolated displacement point (ring interruption). (2) Detected rings are reshaped according to the contour edge computed from the limit parameters. The model obtained is a kind of ideal ring pattern : the limit edge model is scaled down to the ring model scale. Then, the importance of the initial shape is reduced for next detections.

8. Results and Discussion

It should be noticed that we are looking for image intensity extrema. Most of otolith images are properly processed despite marginal structure complexity which tends to squeeze because of otolith growth (old individuals). Actually, the segmentation method used produces a satisfactory enhancement of significant objects allowing a good ring detection and an accurate otolith modelisation (figure 2). All rings are correctly detected even if a small gap between actual and detected extrema persists. A more accurate extrema localization, not yet considered in the processing, should be introduced to overcome this small defect. Between the edge and the last minima, the algorithm detects a maxima corresponding to a very narrow white ring. However, in case of images presenting major defaults, such as interruptions or large spots, the amount of control point likely to drift or to anchor prematurely increases and leads to unexpected fitting (figure 3). Hence, robustness has to be improved and considering otolith growth will increase process reliability for old fish.

9 Conclusion

We have developed a Locally Deformable B-Bubble model which overcomes many problems of existing active contour models and which detects contours in textured noisy and low contrast images. We have applied this new algorithm to the detection of growth rings on fish otoliths by using otolith morphology as a high level information. Results are very encouraging even if the growth process is not yet considered in the processing It will consist to complete high le : information by an a priori knowledge of the growth pattern in order to modulate the amount of control points as wel a SMAX, the maximum displacement step. Otolith centre pointing will be also automated so as to suppress any operat intervention.

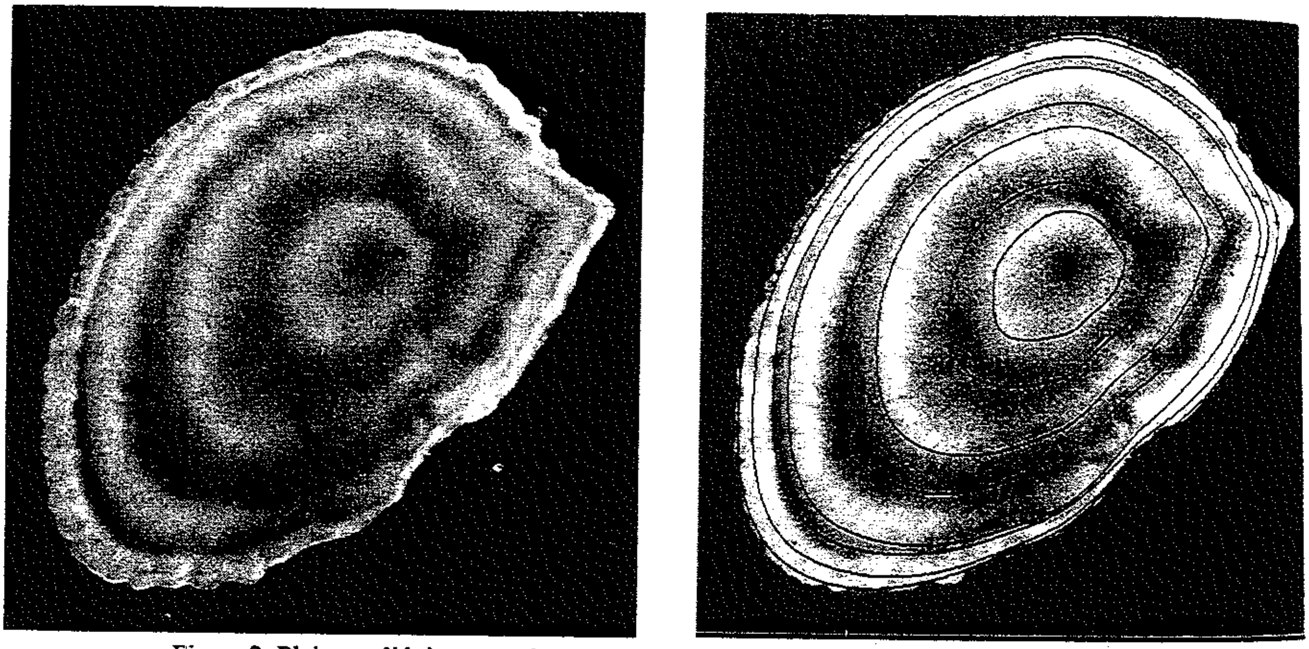

Figure 2: Plaice otolith image and results of our growth ring detection with 16 control points

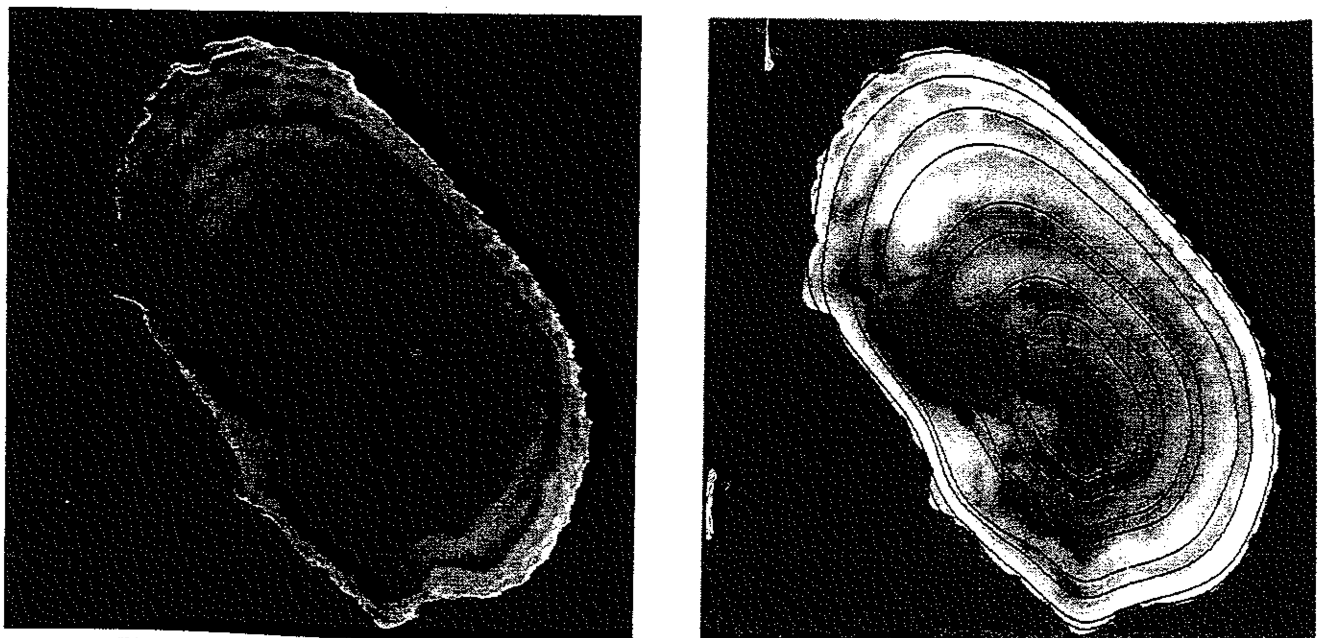

Figure 3: An other plaice otolith image and results of our growth ring detection with 16 control points

References

[1] A. A. Amini, S. Tehrani, and T. E. Weymouth, Using Dynamic Programming for Minimizing the Energy of Active Contours in the presence of Hard Constraints, In: Proceedings, Second International Conference on Computer Vision, 1988, pp. 95-99.

[2] L. D. Cohen, Note on Active Contour Models and Balloons, CVGIP: Image Understanding, March 1991, vol. 53, No. 2, pp. 211-218.

[3] M. Kass, A. Witkin, D. Terzopoulos, Snakes: Active Contour Models, Internatonal Journal of Computer Vision, 1988, 1, pp. 362-385.

[4] J. D. Murray, Mathematical Biology, Springer-Verlag, Second Printing, 1990.

[5] S. Menet, P. S.Marc and G. Medioni, B-snakes: Implementation and application to Stereo, In: Proceedings of Image Understanding Workshop, 1990, pp. 720-726.

[6] H. Troadec, Frequency Demodulation on Otolith Numerical Images for the Automation of Fish Age Estimation, Aquat Living Resour, 1991, 4, pp. 207-219.

[7] R. Tom, Stabilité Structurelle et Morphogenèse, 2eme Edition, Ed. Iterreditions, 1977.

[8] H. C. Welleman & Frank Storbeck, Automatic Ageing of Plaice (Pleuronectes platessa L.) Otoliths by means of Image Analysis, In: Proceedings of the International Otolith Symposium, May 1993, pp. 1-14.

[9] D.J. Williams and M. Shah, A Fast Algorithm for Active Contours and Curvature Estimation, CVGIP: Image Understanding, January 1992, vol. 55, No. 1, pp. 14-26.